

## Rapid synthesis of multifunction composite adsorbent by microwave and evaluate with multiple value integration

Yanlong Sun<sup>a</sup>, Tong Zheng<sup>a,\*</sup>, Guangshan Zhang<sup>a</sup>, Bei Liu<sup>a</sup>, Peng Wang<sup>a,b</sup>, Afed Ullah Khan<sup>a,c</sup>

<sup>a</sup>School of Environment, Harbin Institute of Technology, Harbin 150090, China, Tel. +86 189-0451-3531; email: zhengtong@hit.edu.cn (T. Zheng), Tel. +86 188-4609-0664; emails: llxiaoke@gmail.com (Y. Sun), gszhang@hit.edu.cn (G. Zhang), klliubei@foxmail.com (B. Liu), pwwang73@vip.sina.com (P. Wang), afedullah@yahoo.com (A.U. Khan)

<sup>b</sup>State Key Laboratory of Urban Water Resource and Environment, Harbin Institute of Technology, Harbin 150090, China

<sup>c</sup>Department of Civil Engineering, University of Engineering and Technology, Peshawar, Pakistan

Received 29 November 2017; Accepted 17 June 2018

### ABSTRACT

This work focuses on the synthesis of microwave absorbing-catalytic multifunction novel adsorbent. During adsorbent design secondary pollution produced by adsorbent regeneration is continuously neglected, which motivates the author to load catalyst on adsorbent to enhance the mineralization of adsorbed organic compounds during thermal regeneration. Microwave absorption fuels the synthesis and regeneration of adsorbent. The morphology and structure of composite adsorbent are analyzed by X-ray diffraction, scanning electron microscope-energy dispersive spectrometer, transmission electron microscope, and Brunauer–Emmett–Teller–Barrett–Joyner–Halenda method. The results show that the synthesized composite adsorbent is mesoporous with wide pore diameter distribution and 252 m<sup>2</sup>/g specific surface area. The host of composite adsorbent is  $\gamma$ -Al<sub>2</sub>O<sub>3</sub> and the loaded catalyst is amorphous manganese oxides. The synthesis process of composite adsorbent is designed and evaluated by the response surface methodology using a Box–Behnken design method. After optimization, the optimal adsorption capacity of composite adsorbent can reach up to 135 mg/g, and more than 47% tetracycline can be mineralized into H<sub>2</sub>O and CO<sub>2</sub> during 5 min regeneration. The properties of the composite material can be changed by adjusting synthesis condition. These designed functions of material will make adsorbent more adaptable to meet the growing demand of the environmental standard.

*Keywords:* Adsorbent; Microwave; Catalytic; Regeneration; Mineralization

### 1. Introduction

The water consumption is increasing day by day due to industrial growth. Meanwhile, large amount of wastewater is produced and discharged into rivers [1]. Adsorbents are widely used in wastewater treatment as they are environment-friendly and easy to operate [2,3], especially for in situ ecological remediation.

Many kinds of adsorbent have been developed for wastewater treatment such as activated carbon [4,5], zeolites [1], clay minerals [6], biomaterials [7,8], and metallic oxide. Among these adsorbents, activated carbon is the most commonly used in wastewater treatment processes for its huge specific surface area and excellent adsorption performance [9,10]. However, activated carbon is not stable for thermal regeneration which will cause weight and specific surface area loss. The regeneration process should be conducted in water vapor or carbon dioxide atmosphere because it can be easily oxidized [11,12]. Besides, adsorbed

\* Corresponding author.

organic pollutants may transfer new phase (gas) [13,14]. Therefore,  $\gamma$ - $\text{Al}_2\text{O}_3$  is selected as adsorbent due to its relatively stable physicochemical properties to remove tetracycline from pharmaceutical wastewater. In addition, catalyst is loaded on the adsorbent surface to enhance the oxidization of the adsorbed tetracycline.

Tetracycline antibiotics including tetracycline, oxytetracycline, and chlortetracycline have similar molecular structure and are important antibiotics in animal husbandry [15,16]. Large amount of antibiotics are produced every year to meet the demands of livestock breeding. In the United States, 16 million kilograms of antimicrobial chemicals are consumed each year, for infection treatment and animal growth [17]. The wastewater of tetracycline production contains higher concentration of tetracycline residues which can inhibit the biochemical treatment process. However, the adsorption method can remove the tetracycline residues from the wastewater of tetracycline and solve this problem effectively.

Microwave is used for the synthesis and regeneration of adsorbent due to its high energy density and heating properties. In addition, the synthesis and regeneration process is optimized by response surface methodology (RSM). This research focuses on providing a new prospect for the design and synthesis of novel composite adsorbent which can reduce the secondary pollution of volatile organic compounds during adsorbent regeneration.

## 2. Materials and methods

### 2.1. Chemicals

Tetracycline (99%) is procured from Aladdin Industrial Corporation, Shanghai China, without further purification. Pseudoboehmite is procured from CHINALCO, Shandong, China. Expanded graphite is procured from Ao Yu Graphite Group, Heilongjiang, China. Manganese nitrate, cerous nitrate, barium hydroxide, hydrogen nitrate, oxalic acid, and polyethylene glycol 2000 are all analytical reagent, procured from Xilong Chemical Company, Guangdong, China. Deionized water is used as solvent in all adsorption experiments.

### 2.2. Synthesis and characterization of composite adsorbent

To prepare material precursor, first a certain amount of manganese nitrate and cerous nitrate was weighed and added in 100 mL beaker. After that 10 mL 2% hydrogen nitrate was added in the mixture and stirred at room temperature. Polyethylene glycol 2000 was subsequently added in the mixture solution as pore forming agent. After that expanded graphite was added into the above mixture solution. Finally pseudoboehmite was added into the mixture solution and stirred for 30 min. The precursor was molded into spheres with 3–5 mm diameters and dried at 75°C for 12 h before calcination. Then the precursor spheres were calcined in the modified household microwave oven which can regulate power supply continuously.

Surface morphology of composite adsorbent was observed by transmission electron microscope (TEM) (JEM 1400) and scanning electron microscope-energy dispersive spectrometer (SEM-EDS) (Quanta 200FEG). X-ray diffraction

(XRD) pattern was obtained by max 2550 18 kW Rotating Anode X-ray diffractometer with  $\text{Cu K}\alpha$  ( $k = 1.5418$ ) radiation (40 kV, 300 mA). The samples were scanned in the  $2\theta$  range  $10^\circ$ – $90^\circ$  under continuous mode at a speed of  $10^\circ$   $2\theta/\text{min}$ . Brunauer–Emmett–Teller–Barrett–Joyner–Halenda (BET–BJH) method was used to analyze the surface area and pore size distributions, and it was computed from the data of adsorption isotherm in the relative pressure range of 0.05–0.25.

### 2.3. Adsorbent and regeneration experiments

The adsorption experiments were conducted by putting the synthesized adsorbent into screw-cap vial with a certain tetracycline concentration solution for 24 h and dried the adsorbent after adsorption experiment. The variation of tetracycline concentration during adsorption experiments is tested by UV-vis spectrophotometer (JENWAY-UV 6505) at 355 nm UV wavelength. In regeneration experiments, weigh a certain amount of saturated adsorbent and regenerate the adsorbent in microwave filed with 400 W power supply for 5 min, which can recover 95% adsorption capacity of the synthesized adsorbent. Every regeneration experiment was repeated three times with a blank experiment to avoid the influence of carbon dioxide in air and systematic error. The  $\text{CO}_2$  generated during regeneration is collected by  $\text{Ba}(\text{OH})_2$  solution, using phenolphthalein as indicator and titration with oxalic acid. The test method is reported in former research [18]. The adsorption capacity ( $\eta$ ) and the mineralization percentage ( $\varepsilon$ ) were calculated according to following equations:

$$\eta = \frac{W_t}{W_a} \quad (1)$$

$$\varepsilon = \frac{M_t}{M_o} \times 100\% \quad (2)$$

where  $\eta$  is the adsorption capacity of the composite material,  $W_a$  is the weight of the composite material, and  $W_t$  is the weight of tetracycline adsorbed on the adsorbent.  $\varepsilon$  is mineralization percentage of adsorbed tetracycline,  $M_t$  is the mole of  $\text{CO}_2$  detected in the regeneration process, and  $M_o$  is the mole of carbon atom in adsorbed tetracycline.

### 2.4. Experimental design for optimization by RSM

All the adsorption experiments were conducted in batch mode in the screw-cap vial to avoid systematic error in regeneration experiments. The value range of adsorbent synthesis parameters were chosen based on the adsorbent temperature rising rate in the microwave field and previous research [19,20]. There are three main impact factors in both processes including: microwave power, reaction time, and raw material dose. The optimization of synthesis parameters were developed by Design Expert with RSM and Box–Behnken model. Symbols of the main variables and values of their three coded levels are presented in Table 1.

The relationship between coded and actual values are described based on the following equation:

$$x_i = \frac{(X_i - X_i^*)}{\Delta X_i} \quad (3)$$

Table 1  
Independent variables and coded levels of the synthesis experiments

Variables	Symbol	Coded levels and values		
		-1	0	1
Reaction time (min)	A	3	7	11
Microwave power (W)	B	200	400	600
Material dose (g)	C	4	6	8

where  $x_i$  is the coded value of the independent variable,  $X_i$  is the actual value of the independent variable,  $X_i^*$  is the actual value of the independent variable at the center point, and  $\Delta X_i$  is the step change value.

Each response can be described as a second-order polynomial model to determine the correlation between variables and response. Data is analyzed using analysis of variance. The quadratic equation for each response is shown in the following equation:

$$Y = \beta_0 + \sum_{i=1}^n \beta_i x_i + \sum_{i=1}^n \beta_{ii} x_i^2 + \sum_{i < j} \beta_{ij} x_i x_j \tag{4}$$

where  $Y$  is predicted response and  $\beta_0$  is constant coefficient.  $\beta_i$ ,  $\beta_{ii}$ , and  $\beta_{ij}$  are first-order, second-order, and interaction effects, respectively.  $x_i$  and  $x_j$  are coded independent variables.

### 3. Results and discussion

#### 3.1. Model fitting and statistical analysis

The main objective of RSM in this research is to determine the regression model of the composite material

properties with synthesis conditions. Design Expert 8.05b software is used to design batch synthesis experiments, and quadratic model is used to statistically analyze the relationship among the synthesis conditions and evaluation indexes such as synthesis time, microwave power, the raw material dose, adsorption capacity, and mineralization percentage. The synthesis conditions along with the obtained results of 17 designed experiments are summarized in Table 2. The adsorption capacity of composite adsorbent range from 39.5 to 135.2 mg/g and mineralization percentage of tetracycline during regeneration changed from 8.5% to 47.8%. This result implies that the synthesis conditions significantly influence the adsorption and catalytic properties of synthesized material.

Goodness of model fit will ensure the adequacy of the employed model. The significance of quadratic regression model and parameters affecting the process is tested by the values of  $F$  and  $P$ . Analysis of variance results are summarized in Table 3. Generally, the values of  $P$  less than 0.05 indicated that model terms are significant, whereas the values greater than 0.1 are usually considered as insignificant [20]. In addition, adequate precision measures in predicted response is relative to its associated error, and the value greater than 4.0 is desirable [22].

Table 3 presents the details of ANOVA and the status of the parameters. The  $F$  value of model is 26.80 for adsorption capacity and 8.25 for mineralization percentage implied that the model is significant. There is only 0.01% chance that a “Model  $F$ -Value” is due to noise. Furthermore,  $P$  values of two models are less than 0.05 at 95% confidence level, which shows that the models are statistically significant. The results also suggest that the data is well described by quadratic model and can be efficiently applied in these systems. Besides,  $A$ ,  $B$ ,  $C$ ,  $AB$ ,  $A^2$ , and  $B^2$  are significant for adsorption property model terms, while  $A$ ,  $B$ ,  $C$ , and  $AB$  are significant for catalytic property model terms.

Table 2  
Experimental results of the synthesis process

Std.	Run.	Time (min)	Power (W)	Dose (g)	Adsorption capacity (mg/g)	Mineralization percentage
1	5	3	200	6	39.5	47.8
2	2	11	200	6	106.3	13.9
3	12	3	600	6	108.3	17.0
4	3	11	600	6	132.7	18.7
5	15	3	400	4	82.0	20.1
6	4	11	400	4	117.5	8.5
7	1	3	400	8	97.7	28.4
8	8	11	400	8	135.2	19.8
9	16	7	200	4	79.5	19.0
10	11	7	600	4	126.0	17.8
11	9	7	200	8	87.6	24.2
12	17	7	600	8	129.1	14.5
13	13	7	400	6	107	16.9
14	7	7	400	6	112.4	15.5
15	10	7	400	6	117.5	18.3
16	6	7	400	6	118.0	17.9
17	14	7	400	6	110.0	19.8

Table 3  
ANOVA table from Box–Behnken model of synthesized composite adsorbent

Source	DF <sup>a</sup>	Adsorption capacity			Mineralization percentage		
		F-Value	P-Value	Status	F-Value	P-Value	Status
Model	9	26.80	<0.0001	Significant	8.25	0.0055	Significant
A	1	117.90	<0.0001	Significant	25.04	0.0016	Significant
B	1	146.76	<0.0001	Significant	12.42	0.0097	Significant
C	1	8.70	0.0214	Significant	6.22	0.0492	Significant
AB	1	15.72	0.0054	Significant	23.11	0.0019	Significant
AC	1	0.035	0.8569	Not significant	0.16	0.6975	Not significant
BC	1	0.22	0.6543	Not significant	1.32	0.2887	Not significant
A <sup>2</sup>	1	6.94	0.0337	Significant	3.76	0.0938	Not significant
B <sup>2</sup>	1	13.06	0.0086	Significant	3.09	0.1221	Not significant
C <sup>2</sup>	1	0.58	0.4710	Not significant	1.20	0.3093	Not significant
Lack of fit	3	1.61	0.3203	Not significant	11.10	0.0208	Significant

<sup>a</sup>Degree of freedom.

According to the batch mode experiments data (shown in Table 2), final empirical models of composite adsorbent adsorption and catalytic properties with synthesis conditions are described by the following equations, respectively:

$$Y_1 = 112.98 + 20.53A + 22.90B + 5.57C - 10.60A \times B - 0.50A \times C - 1.25B \times C - 6.87A^2 - 9.41B^2 + 1.98C^2 \quad (5)$$

$$Y_2 = 17.68 - 6.55A - 4.61B + 2.69C + 8.90A \times B + 0.75A \times C - 2.13B \times C + 3.50A^2 + 3.17B^2 - 1.98C^2 \quad (6)$$

where  $Y_1$  and  $Y_2$  are the predicted response (adsorption capacity and mineralization percentage, respectively),  $A$ ,  $B$ , and  $C$  are the coded values of synthesis time, microwave power, and raw material dose, respectively.

The values of the correlation coefficient ( $R^2$ ) and adjusted correlation coefficient (Adj.  $R^2$ ) of Eqs. (3) and (4) are found to be 0.9780 and 0.9139 and 0.9496 and 0.8032, respectively. This indicates that experimental data agree well with the model predicted values. Besides, adequate precision values of the models are 22.44 and 12.39 which are greater than 4 indicating that the noise ratio is low and the models can be used to navigate the design space.

### 3.2. Effect of interactive variables and 3D response surface plot

To evaluate the simultaneous mutual impact of the three main synthesis condition on the considered responses, three-dimensional (3D) response surface plots are employed to estimate response values. The results are shown in Fig. 1.

Figs. 1(a) and (b) are the response surface plots of the effect of microwave power and irradiation time on the adsorption and catalytic properties, respectively. It can be observed that the adsorption capacity of the synthesized adsorbent increases with the microwave power and irradiation time. However, the mineralization percentage of tetracycline decreases. Higher microwave power can provide

higher synthesis temperature which fuel the transformation of pseudoboehmite to  $\gamma$ - $\text{Al}_2\text{O}_3$ , and adequate reaction time is necessary for the formation of material porous structure [23,24]. The catalyst loaded on adsorbent surface is also formed during this process. Whereas amorphous manganese oxides has better catalytic properties as the growth of manganese oxides will decrease its dispersion on the adsorbent surface [25,26]. Furthermore, the dose of raw material also impacts the precursor temperature rise process in microwave field, as the microwave provides energy field not temperature field.

To a certain extent, increasing raw material dose is beneficial for improving microwave absorbing efficiency. Besides, it can also decrease the material temperature rising rate which can avoid uneven heating. Figs. 1(c)–(f) illustrate the mutual interactive effect of raw material dose with microwave power and irradiation time. The contour lines patterns of tetracycline adsorption are denser than the mineralization percentage patterns. It suggests that the adsorption property of synthesized material is more influential than catalytic property when change in the synthesis condition. Similarly, the effect of microwave power and synthesis time on adsorption and catalytic property is more remarkable than that of adsorbent dose.

### 3.3. Optimization

Ideal condition for the synthesis of composite adsorbent is determined by change of adsorption capacity and mineralization percentage of tetracycline base on design master programming. The optimum synthesis condition of adsorbent with maximum adsorption capacity is microwave power 506.5 W, synthesis time 10.22 min, and adsorbent dose 7.54 g. Under this condition the adsorption capacity of synthesized adsorbent can reach 135 mg/g. Besides, the optimum synthesis condition of adsorbent with optimal catalytic property is under microwave power 200.0 W, synthesis time 3.0 min, and adsorbent dose 8.0 g. Under this condition

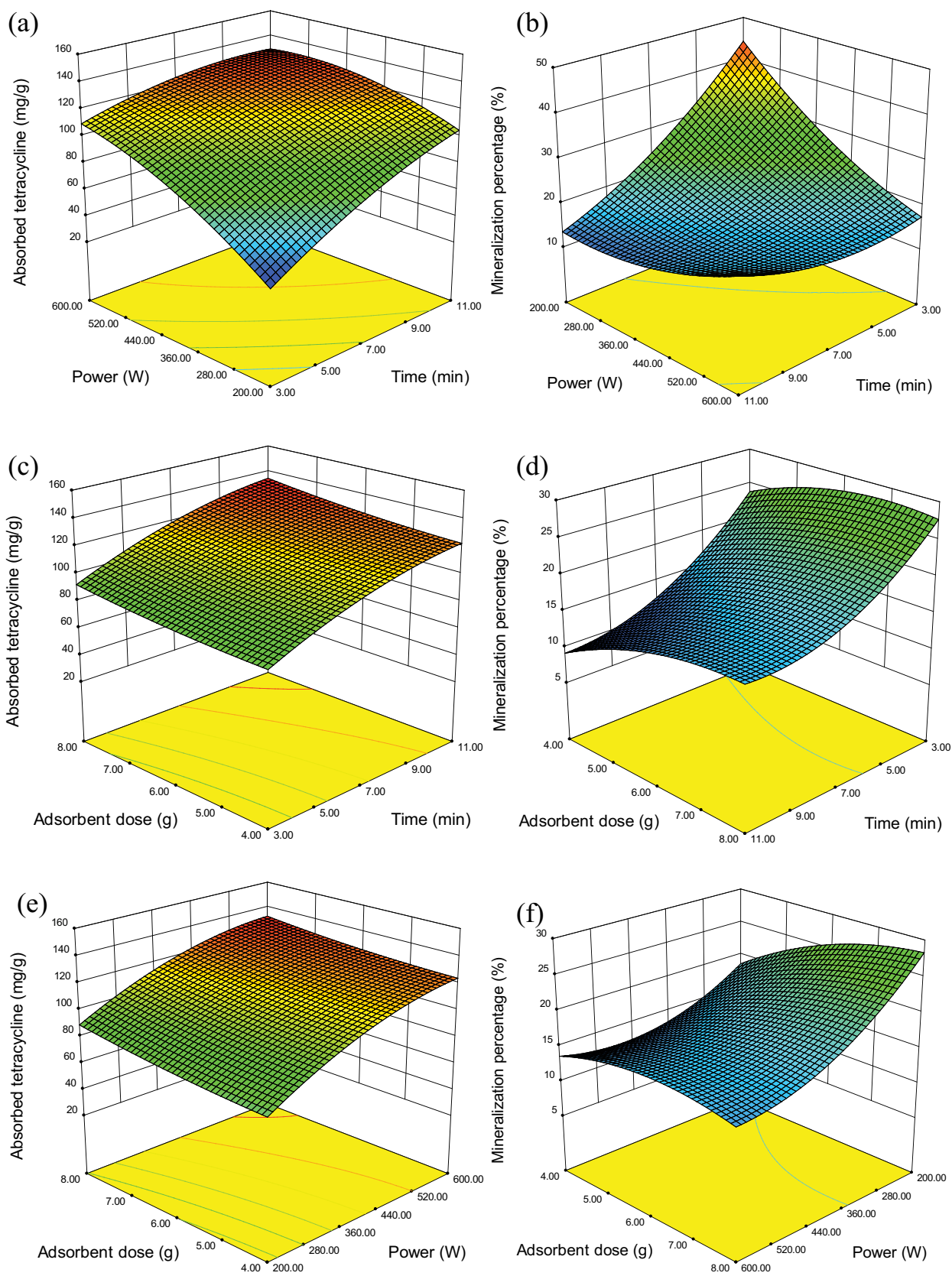


Fig. 1. 3D response plots for the effect of interaction on adsorption property ((a), (c), and (e)) and catalytic property ((b), (d), and (f)).

the synthesized adsorbent can mineralize more than 47% tetracycline during regeneration. As it is multiresponse optimization, the synthesis condition for maximum adsorption capacity is not consistent with the maximum mineralization percentage condition. To obtain optimum synthesis condition, the adsorption capacity of composite material is primarily considered as it is more sensitive to changes in synthesis condition. Therefore, mineralization percentage is optimized based on the adsorption capacity results. The ideal condition based on the regression model is microwave power 400–500 W, synthesis time 6.5–7.5 min, and adsorbent dose 7.5–8 g. Under this condition, the adsorption capacity of the synthesized adsorbent is around 120 mg/g, and the mineralization percentage of tetracycline can reach 20% after 5 min regeneration.

### 3.4. Characterizations of the synthesized composite adsorbent

XRD characterization is used to confirm the structure of composite adsorbent. The results of XRD test are shown in Fig. 2. There is very strong diffraction peak at  $26.5^\circ$  which corresponds to the (002) plane of expanded graphite (JCPDS no. 89-8487). Expanded graphite has layer structure and can widen pore distribution of synthesized adsorbent. It is beneficial for internal diffusion of the organic pollutants in water. Fig. 2 also shows the wide-angle XRD peaks located at  $2\theta = 36.9^\circ, 39.2^\circ, 45.4^\circ,$  and  $66.7^\circ$  that correspond to the (311), (222), (400), and (440) planes of  $\gamma\text{-Al}_2\text{O}_3$  (JCPDS no. 04-858), respectively [19].

The broad peaks in composite adsorbent XRD pattern reflect that the crystallinity degree of  $\gamma\text{-Al}_2\text{O}_3$  in composite adsorbent is lower than the expanded graphite. The main reason behind that is the unit cell of expanded graphite which is formed before the synthesis process. However, the  $\gamma\text{-Al}_2\text{O}_3$  in composite adsorbent is transformed from pseudoboehmite in a few minutes in microwave field. The short synthesis time limits the crystallization of  $\gamma\text{-Al}_2\text{O}_3$ , which is beneficial for

the development of mesoporous structure and big specific area of composite adsorbent [19,27]. The specific surface area of synthesized material is determined by BET method whose results are shown on Fig. 4. The XRD test illustrates that the composite adsorbent can be formed in the microwave field in a few minutes.

Pervious characterization demonstrates the crystal structure of synthesized composite adsorbent. Microscopy (TEM and SEM) studies are used to learn more about the morphology and the dispersion of expanded graphite in composite adsorbent. SEM image in Fig. 3(a) shows that the synthesized composite adsorbent has macropore structure. In addition, expanded graphite is also observed which adhere on the surface of  $\gamma\text{-Al}_2\text{O}_3$ . The uniform distribution and tight junction of the two materials in SEM pattern can improve the heat transfer efficiency during the synthesis and regeneration process of composite adsorbent. Moreover, it can avoid local overheating which can cause phase transformation of  $\gamma\text{-Al}_2\text{O}_3$  which can improve the adsorption properties of the synthesized adsorbent [28].

TEM images in Figs. 3(c) and (d) clearly show the porous structure of composite adsorbent. The synthesized composite adsorbent is composed of expanded graphite and  $\gamma\text{-Al}_2\text{O}_3$  particles (5–10  $\mu\text{m}$ ), which are composed of smaller porous  $\gamma\text{-Al}_2\text{O}_3$  particles (around 300 nm). The secondary particle constructs the macropore which are beneficial for the intraparticle diffusion of pollutants in adsorbent. In addition, the mesopore of small  $\gamma\text{-Al}_2\text{O}_3$  particles can provide abundant adsorbent site. Furthermore, manganese and cerium are detected by EDS test. The detail elements ratio of composite adsorbent is listed in Table 4. The actual atom ratio of Al, Mn, and Ce are tabulated in Table 4 approaching to the raw material atom ratio (Al:Mn:Ce = 100:5:1), which proved that the catalyst has been loaded on the surface of the adsorbent. However, there are no catalyst peaks observed in the XRD pattern in Fig. 2, which indicates that the catalyst is amorphous.

The nitrogen adsorption–desorption isotherms and BJH pore-size distribution of composite adsorbent are shown in Fig. 4. The curve of composite adsorbent exhibits a typical mesoporous structure, as the isotherm curve exhibits a type IV isotherm with H1 hysteresis loop. Type IV isotherm which has a hysteresis loop is occurred due to capillary condensation of nitrogen gas in the pore, which indicates that there is a narrow pore size distribution in the sample [29]. BET surface area and pore volume of synthesized composite adsorbent are 252 and 0.86  $\text{m}^3/\text{g}$  respectively. It is close to the relative study, even the synthesis time is only a few minutes in this study [20,23,27]. BJH average pore diameter distribution of synthesized composite adsorbent is wide and the pore-size distribution curve includes two peaks. It indicates that the

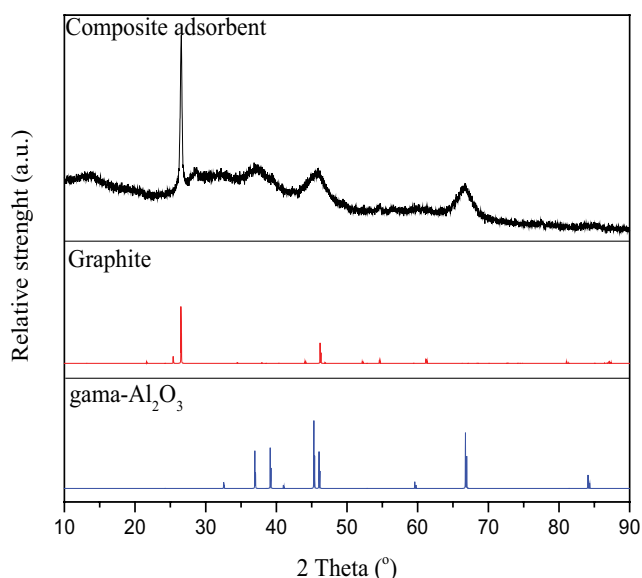


Fig. 2. XRD pattern of composite adsorbent synthesized by microwave.

Table 4  
EDS result of composite adsorbent

Element	Wt%	At%
Al	43.54	31.05
Mn	4.17	1.46
Ce	1.87	0.26
C	16.52	26.46

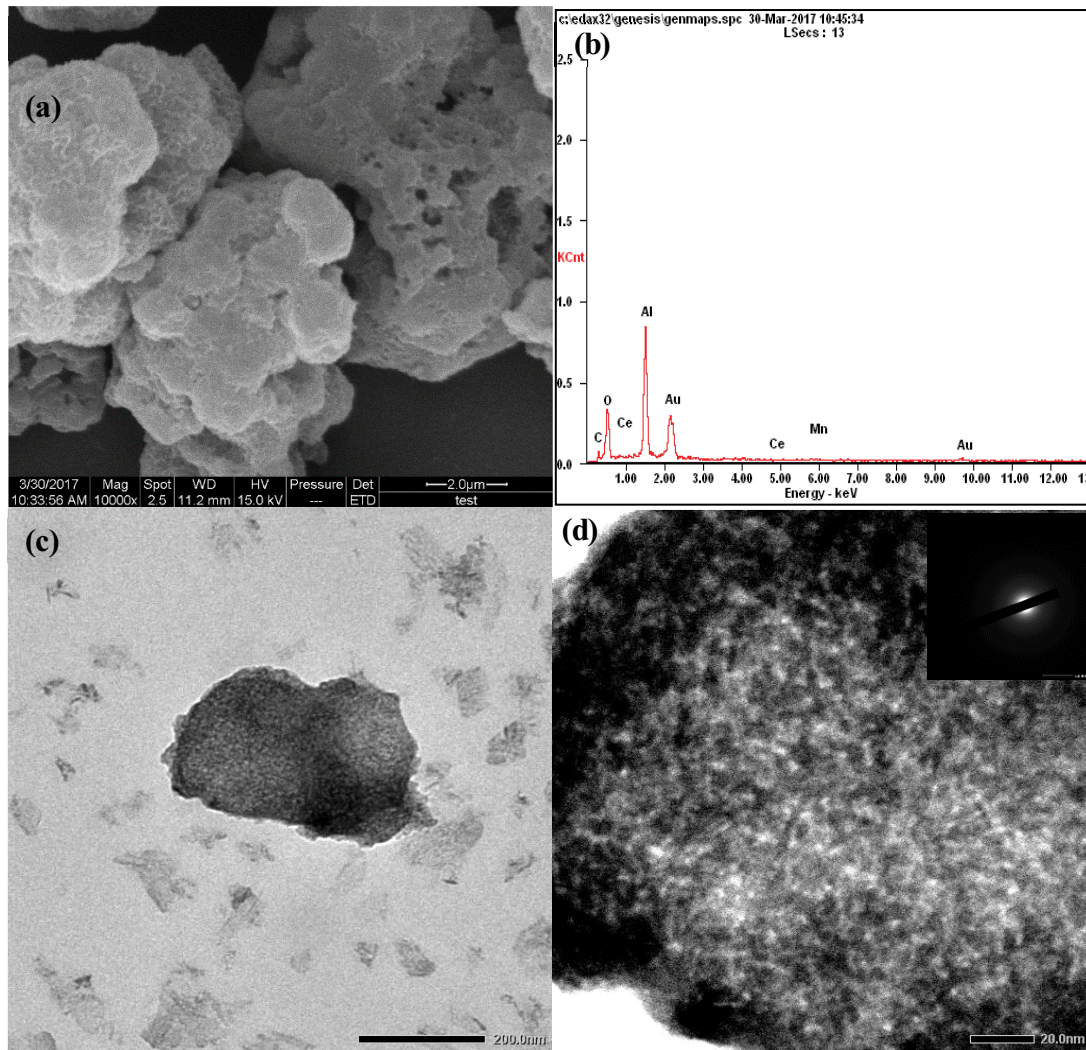


Fig. 3. SEM image (a), EDS image (b), and TEM images ((c) and (d)) of composite adsorbent.

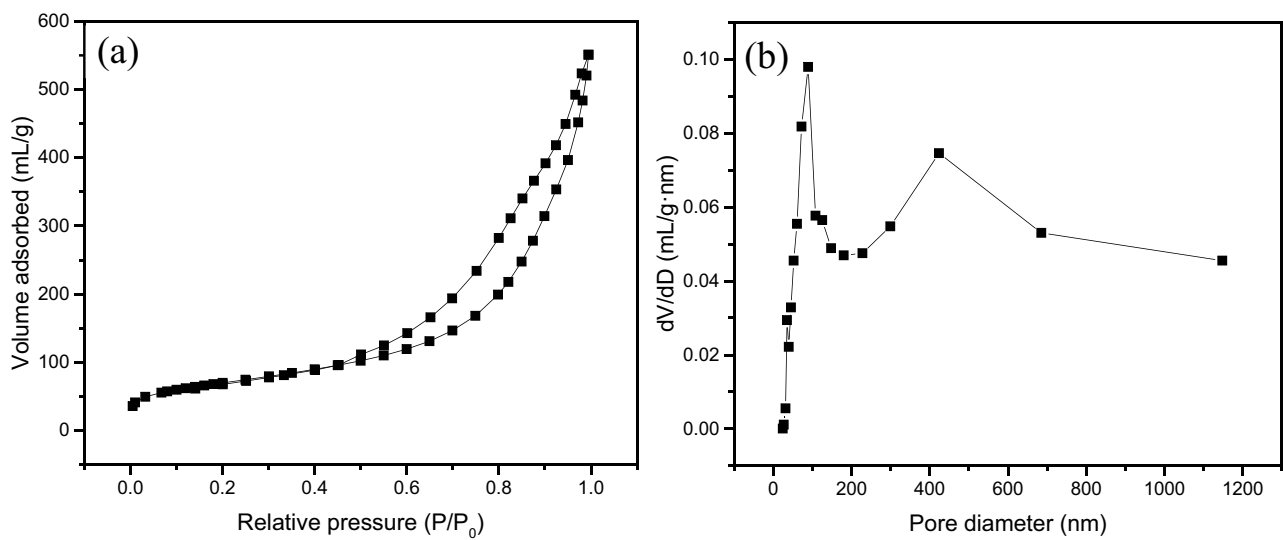


Fig. 4. Nitrogen adsorption–desorption isotherms (a) and pore diameter distribution of composite adsorbent (b).

composite adsorbent has two pore-size distribution of 20–140 and 230–680 nm. The pore size distribution results corresponding morphology characterization are shown in Fig. 3. The small pores in material provide a large surface area and abundant active sites, while the large pore of synthesized material provides suitable space for reaction and diffusion of pollutants. It is well founded knowledge that the bigger pore diameter and larger pore volume are beneficial for the reaction between the adsorbent and compounds in liquid phase [30–32].

#### 4. Conclusion

In this study, multifunctional composite adsorbent is synthesized by microwave heating method. The morphology and structure characterization results show that the synthesized composite material has big specific surface area and wide pore diameter distribution. The host material of the synthesized material is  $\gamma$ - $\text{Al}_2\text{O}_3$  and amorphous manganese oxides are loaded on surface of host material. RSM is used to optimize the rapid synthesized process. The constructed regression models show that the optimum preparation condition for composite material is 7.5–8 g raw material irradiated under 400–500 W microwave power for 6.5–7.5 min. At this condition, the adsorption capacity of the synthesized adsorbent is around 120 mg/g and the mineralization percentage of tetracycline can reach 20% after 5 min regeneration (will be higher after optimizing the regeneration process). In addition, the properties of the composite material are regular for the practical application demand. These results show the novelty of multifunction composite adsorbent which has both absorption and catalytic properties and can be rapidly synthesized or regenerated.

#### Acknowledgments

We are thankful to the financial assistance of Science Foundation of Heilongjiang Province [grant no. B2016005]; National Natural Science Foundation of China [grant no. 51678185]; Fundamental Research Funds for the Central Universities [Grant no. HIT.NSRIF.2017060].

#### References

- [1] S. Wang, Y. Peng, Natural zeolites as effective adsorbents in water and wastewater treatment, *Chem. Eng. J.*, 156 (2010) 11–24.
- [2] Z. Yu, S. Peldszus, P.M. Huck, Adsorption of selected pharmaceuticals and an endocrine disrupting compound by granular activated carbon. 1. Adsorption capacity and kinetics, *Environ. Sci. Technol.*, 43 (2009) 1467–1473.
- [3] L. Zhang, H. Jiang, C. Ma, D. Yong, Microwave regeneration characteristics of activated carbon for flue gas desulfurization, *J. Fuel Chem. Technol.*, 40 (2012) 1366–1371.
- [4] D. Menard, X. Py, N. Mazet, Activated carbon monolith of high thermal conductivity for adsorption processes improvement: Part B Thermal regeneration, *Chem. Eng. Process*, 46 (2007) 565–572.
- [5] J. Jaramillo, P.M. Álvarez, V. Gómez-Serrano, Preparation and ozone-surface modification of activated carbon. Thermal stability of oxygen surface groups, *Appl. Surf. Sci.*, 256 (2010) 5232–5236.
- [6] P. Chang, Z. Li, T. Yu, S. Munkhbayer, T. Kuo, Y. Hung, J. Jean, K. Lin, Sorptive removal of tetracycline from water by palygorskite, *J. Hazard. Mater.*, 165 (2009) 148–155.
- [7] Z. Du, T. Zheng, P. Wang, L. Hao, Y. Wang, Fast microwave-assisted preparation of a low-cost and recyclable carboxyl modified lignocellulose-biomass jute fiber for enhanced heavy metal removal from water, *Bioresour. Technol.*, 201 (2016) 41–49.
- [8] J. Rivera-Utrilla, C.V. Gómez-Pacheco, M. Sánchez-Polo, J.J. López-Peñalver, R. Ocampo-Pérez, Tetracycline removal from water by adsorption/bioadsorption on activated carbons and sludge-derived adsorbents, *J. Environ. Manage.*, 131 (2013) 16–24.
- [9] V. Rakić, V. Rac, M. Krmar, O. Otman, A. Auroux, The adsorption of pharmaceutically active compounds from aqueous solutions onto activated carbons, *J. Hazard. Mater.*, 282 (2015) 141–149.
- [10] M. Kwiatkowski, E. Broniek, Application of the LBET class adsorption models to the analysis of microporous structure of the active carbons produced from biomass by chemical activation with the use of potassium carbonate, *Colloids Surf., A*, 427 (2013) 47–52.
- [11] X. Han, H. Lin, Y. Zheng, Regeneration methods to restore carbon adsorptive capacity of dibenzothiophene and neutral nitrogen heteroaromatic compounds, *Chem. Eng. J.*, 243 (2014) 315–325.
- [12] C. Moreno-Castilla, 96/03476–Thermal regeneration of an activated carbon exhausted with different substituted phenols, *Fuel Energy Abstr.*, 37 (1996) 1417–1423.
- [13] J. Chen, Z. Cheng, Y. Jiang, L. Zhang, Direct VUV photo-degradation of gaseous-pinene in a spiral quartz reactor: intermediates, mechanism, and toxicity/biodegradability assessment, *Chemosphere*, 81 (2010) 1053–1060.
- [14] Y. Sun, B. Zhang, T. Zheng, P. Wang, Regeneration of activated carbon saturated with chloramphenicol by microwave and ultraviolet irradiation, *Chem. Eng. J.*, 320 (2017) 264–270.
- [15] A.K. Sarmah, M.T. Meyer, A.B. Boxall, A global perspective on the use, sales, exposure pathways, occurrence, fate and effects of veterinary antibiotics (VAs) in the environment, *Chemosphere*, 65 (2006) 725.
- [16] K. Kümmerer, Antibiotics in the environment, *Upsala J. Med. Sci.*, 119 (2008) 108.
- [17] A.G. King, Research advances: eating clay?; Look to soil for new leads in arthritis treatment; the fate of tetracyclines, *J. Chem. Educ.*, 83 (2006) 3.
- [18] O. Bajt, G. Mailhot, M. Bolte, Degradation of dibutyl phthalate by homogeneous photocatalysis with Fe(III) in aqueous solution, *Appl. Catal., B*, 33 (2001) 239–248.
- [19] W. Wang, K. Zhang, Y. Yang, H. Liu, Z. Qiao, H. Luo, Synthesis of mesoporous  $\text{Al}_2\text{O}_3$  with large surface area and large pore diameter by improved precipitation method, *Microporous Mesoporous Mater.*, 193 (2014) 47–53.
- [20] S. Lan, N. Guo, L. Liu, X. Wu, L. Li, S. Gan, Facile preparation of hierarchical hollow structure gamma alumina and a study of its adsorption capacity, *Appl. Surf. Sci.*, 283 (2013) 1032–1040.
- [21] I. Arslan-Alaton, G. Tureli, T. Olmez-Hanci, Treatment of azo dye production wastewaters using photo-Fenton-like advanced oxidation processes: optimization by response surface methodology, *J. Photochem. Photobiol., A*, 202 (2009) 142–153.
- [22] N. Aghamohammadi, H.B. Aziz, M.H. Isa, A.A. Zinatizadeh, Powdered activated carbon augmented activated sludge process for treatment of semi-aerobic landfill leachate using response surface methodology, *Bioresour. Technol.*, 98 (2007) 3570–3578.
- [23] C.L.L. de Faria, T.K.R. de Oliveira, V.L. Dos Santos, C.A. Rosa, J.D. Ardisson, W.A. de Almeida Macêdo, A. Santos, Usage of the sol-gel process on the fabrication of macroporous adsorbent activated-gamma alumina spheres, *Microporous Mesoporous Mater.*, 120 (2009) 228–238.
- [24] Q. Liu, A. Wang, X. Wang, T. Zhang, Morphologically controlled synthesis of mesoporous alumina, *Microporous Mesoporous Mater.*, 100 (2007) 35–44.
- [25] X. Wang, Y. Guo, G. Lu, Y. Hu, L. Jiang, Y. Guo, Z. Zhang, An excellent support of Pd catalyst for methane combustion: thermal-stable Si-doped alumina, *Catal. Today*, 126 (2007) 369–374.



- [26] A.L. Kustov, M. Makkee, Application of NOX storage/release materials based on alkali-earth oxides supported on  $\text{Al}_2\text{O}_3$  for high-temperature diesel soot oxidation, *Appl. Catal., B*, 88 (2009) 263–271.
- [27] B. Huang, C.H. Bartholomew, B.F. Woodfield, Facile synthesis of mesoporous  $\gamma$ -alumina with tunable pore size: the effects of water to aluminum molar ratio in hydrolysis of aluminum alkoxides, *Microporous Mesoporous Mater.*, 183 (2014) 37–47.
- [28] R.A. Mayanovic, H. Yan, A.D. Brandt, Z. Wang, M. Mandal, K. Landskron, W.A. Bassett, Mechanical and hydrothermal stability of mesoporous materials at extreme conditions, *Microporous Mesoporous Mater.*, 195 (2014) 161–166.
- [29] S.J. Gregg, K.S.W. Sing, *Adsorption, Surface Area, and Porosity*, Academic Press, 1982.
- [30] H. Ma, J. Shen, S. Min, L. Xin, Z. Li, L. Yu, L. Na, M. Ye, Significant enhanced performance for Rhodamine B, phenol and Cr(VI) removal by  $\text{Bi}_2\text{WO}_6$  nanocomposites via reduced graphene oxide modification, *Appl. Catal., B*, 121–122 (2012) 198–205.
- [31] X. Li, D. Han, Y. Xu, X. Liu, Z. Yan, Bimodal mesoporous  $\gamma$ - $\text{Al}_2\text{O}_3$ : a promising support for CoMo-based catalyst in hydrodesulfurization of 4,6-DMDBT, *Mater. Lett.*, 65 (2011) 1765–1767.
- [32] X.M. Liu, H.X. Xue, X. Li, Z.F. Yan, Synthesis and hydrodesulfurization performance of hierarchical mesopores alumina, *Catal. Today*, 158 (2010) 446–451.